ELECTROHYDRODYNAMIC INSTABILITY IN NEMATIC LIQUID CRYSTAL BORDERING WITH CYLINDRICAL ANODIZED ALUMINUM OXIDE NANOPORES

Sh.O. EMINOV, G.F. GANIZADE, I.I. GURBANOV, A.R. IMAMALIYEV, A.X. KARIMOVA, A.A. RAJABLI

Ministry of Science and Education of Azerbaijan, Institute of Physics,
H. Javid av.13I, Baku, AZ1143, Azerbaijan
E-mail: Rahimoglu@mail.ru

Using the liquid crystal 4-methoxybenzylidene)-4'-butylaniline (MBBA) as an example, it is shown that in an electrooptic cell where surface of an indium teen oxide (ITO) electrode is coated with cylindrical anodized aluminum oxide (AAO) nanoporous, unwanted current effects such as electrohydrodynamic instabilitiy emerging at high voltages can be avoided, which is important for display applications of liquid crystals with negative dielectric anisotropy.

INTRODUCTION

The behavior of liquid crystals in confined small volumes attracts great scientific attention [1-5]. Due to the unique competition of surface and elastic forces, a number of structures (singularities and defects) are observed in such systems, which are characterized by a certain director distribution. These structures can be controlled to a certain extent by varying the interface material (polymer, metal, semiconductor [6]), shape (spherical [7, 8], cylindrical [9,10]) and small volume size (micropores [11,12], nanopores [13]), phase (nematic, smectic, cholesteric [14, 15]) of the liquid crystal, sign and magnitude of the dielectric anisotropy of the liquid crystal [16]. Examples of applications include flexible displays based on polymer-dispersed liquid crystals, which are micron-sized liquid crystal droplets distributed in a polymer matrix [17-19].

Nanoporous anodized aluminum oxide (AAO) film, which contains many cylindrical pores of nanoscale diameter (20-100 nm) and length (500 nm-50 μm) oriented parallel to each other and arranged strictly perpendicular to the substrate surface, is a suitable basis for the realization of various structures in terms of practical applications [20-27]. Membranes based on AAO, due to good electrophysical and optical properties, as well as the ability to easily obtain through capillary nanochannels and change their geometric parameters (diameter and length), are widely used in a variety of fields: micro- and ultrafiltration, for the manufacture of sensors, bacterial analysis by fluorescence optical microscopy, etc. They are also widely used as a template for the synthesis of various nanostructures and devices on their basis [22-24]. Among other applications of AAO, the use of perfectly ordered porous aluminum oxide to fabricate two-dimensional (2D) photonic crystals [21] is of considerable interest. They possess a spatially periodic refractive index with a lattice constant of the same order as the wavelength of light, and potential scientific and technological applications based on their unique light transmission properties. Porous aluminum oxide is useful in terms of forming a porous matrix structure with high aspect ratio, which cannot be achieved by conventional processes such as electron beam lithography [25].

In recently published works it is proposed to use cylindrical nanopores on the basis of AAO as a substrate to obtain reliable qualitative homeotropic orientation in case of realization of the B-effect in liquid crystals with negative dielectric anisotropy [26-29]. When such liquid crystals are used in displays with active addressing, sufficiently high voltages are applied to the pixels, at which undesirable current effects in the form of electrohydrodynamic instabilities (EHDI) can occur. To help solve this problem, in the presented work we studied the influence of AAO on the threshold of occurrence and cutoff frequency of electrohydrodynamic instability (EHDI) for liquid crystal MBBA.

EXPERIMENT

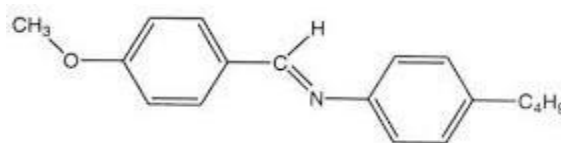*N*-(4-Methoxybenzylidene)–4–butylaniline (MBBA)

Fig. 1

is a classic LC whose properties can be found in most well-known liquid crystal textbooks [16]. MBBA exhibits a nematic phase in the temperature range from 16 ºC to 45 ºC. Due to polar groups -C-O-C- at the end of the molecule and -CH=N- in the backbone, MBBA has negative anisotropy of dielectric permittivity, i.e. dielectric permittivity along the long axis of the molecules ($\varepsilon_\parallel$) is less than dielectric permittivity in the direction perpendicular to the long axis of the molecules ($\varepsilon_\perp$). At room temperature $\Delta\varepsilon = \varepsilon_\parallel - \varepsilon_\perp = 4.75 - 5.4 = -0,65$.

The scheme of fabrication of glass/indium teen oxide/aluminum oxide (glass/ITO/AO) structures begins with the fact that a thin aluminum film with a thickness in the range from 300 to 500 nm was deposited to the previously obtained ITO layer in the vacuum chamber of the Leybold Heraeus-Z550 radio-frequency magnetron sputtering unit equipped with a turbomolecular vacuum pump using a titanium target. Anodization of aluminum film was carried out in a self-contained two-electrode electrochemical cell in which an Al/ITO/glass structure with a operating area of 3x2 cm^2 was connected to the anode and a platinum plate to the cathode. The electrolyte was 4% aqueous oxalic acid solution ($H_2C_2O_4$) and the electrolyte temperature was maintained at 4.0 ±0.5°C with vigorous stirring (300 s^{-1}) by a micro propeller. The anodization voltage was maintained at 40 V in potentiostatic mode and the anodization current was recorded by a digital sensor HANTEK 315B. After anodization, the structure was annealed at 250 ºC in order to crystallize the ITO film, which usually has an amorphous structure after magnetron sputtering, as well as to remove excess water from the hydrolysis products from the AAO.

Frontal and lateral SEM images of the obtained film are presented in Fig.2.
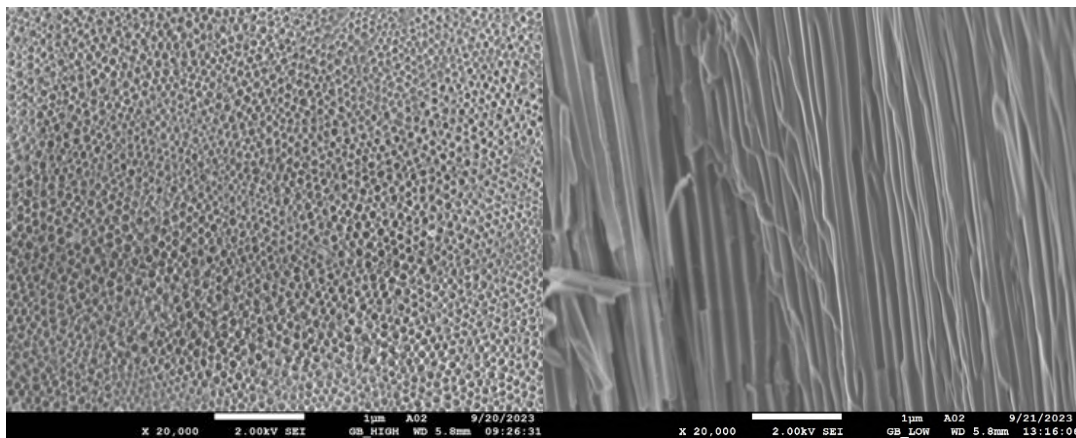
a)   b)

Fig.2

Based on spectrophotometric measurements (Fig.3), the thickness of the AAO layer can be determined. It is approximately equal to 1.2 μm.
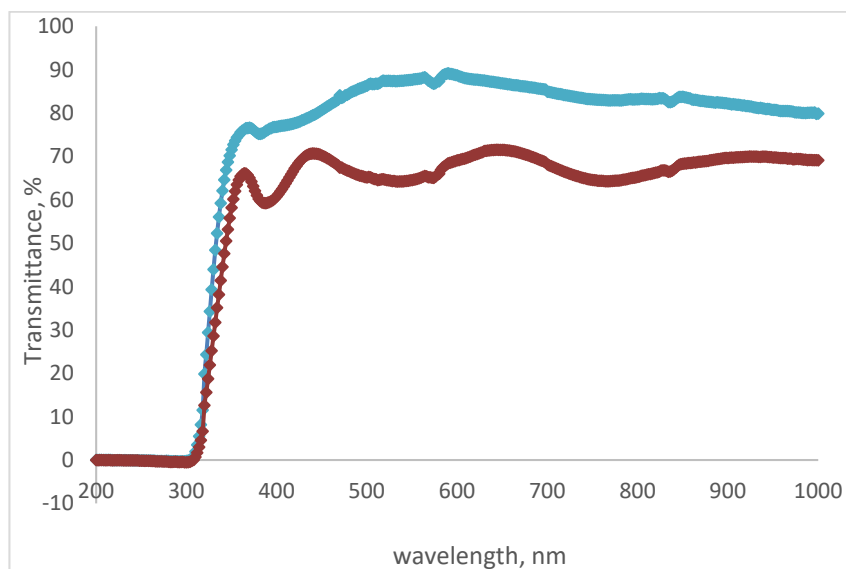

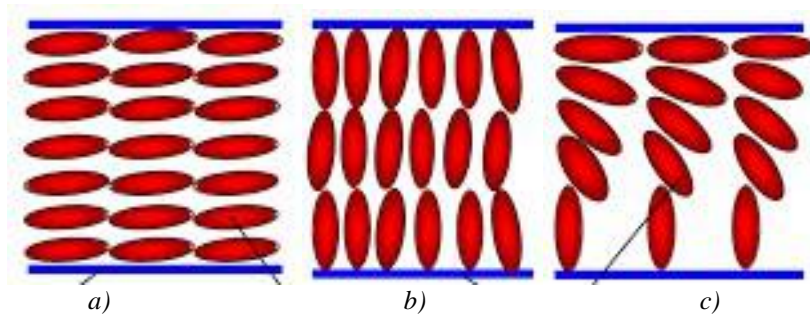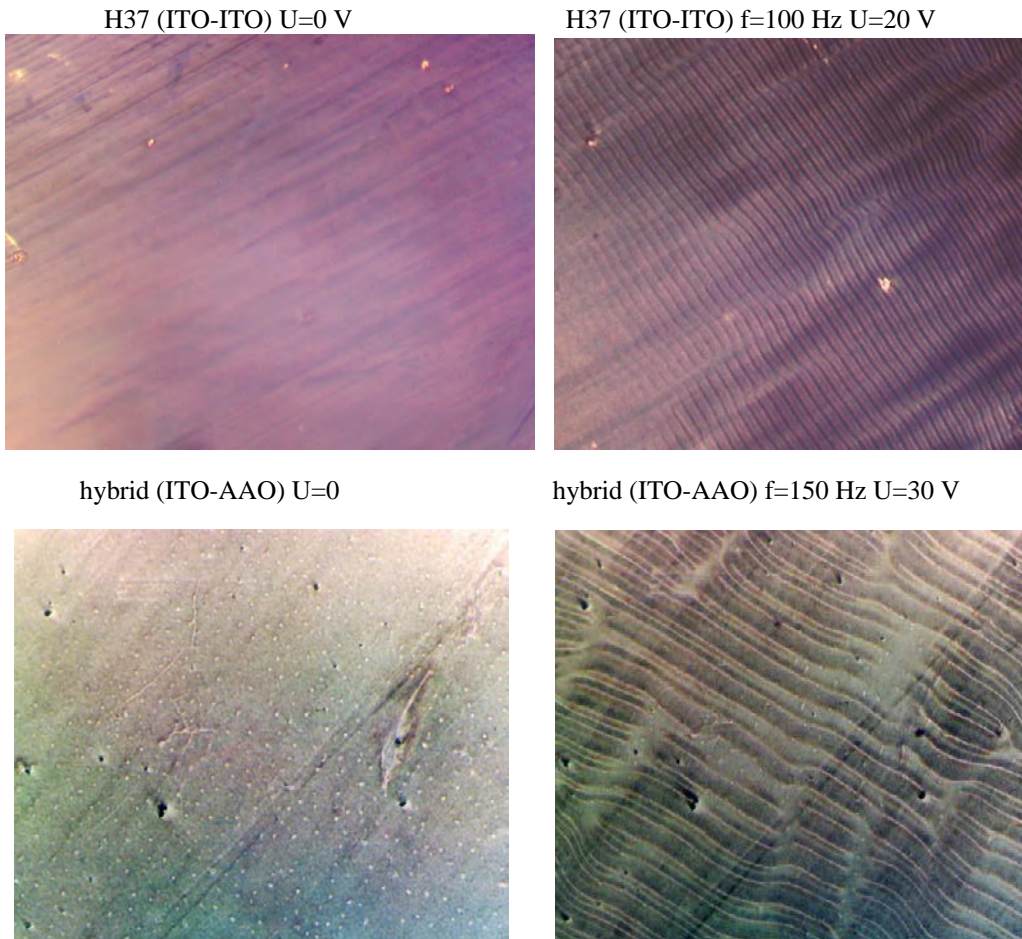*Fig.3*

a)   *b)*   *c)*

Fig. 4

The measurements were carried out in a cell consisting of two plane-parallel glass plates, the inner surfaces of which are coated with a transparent layer of ITO or AAO oxides. The untreated ITO layer gives a good planar orientation for MBBA, and AAO gives a qualitative homeotropic orientation. Thus, if the LC is bordered on both sides by ITO, a planar texture is obtained (Fig. 4a). If the LC is bordered on both sides by AAO, a homeotropic texture will result (Fig. 4b). If the LC is bounded by ITO on one side and AAO on the other side, a hybrid texture is obtained (Fig. 4c).

The thickness of the LC layer was fixed by special Teflon spacers with a thickness of 30 μm. Cells were filled in vacuum by capillary method in isotropic phase of LC. Measurements were carried out at a temperature of 23 ºC.

The electric field was applied to the LC cell using a G3-109 sinusoidal voltage generator, and the structural changes in the liquid crystal were observed in a KARL ZEISS JENA polarization microscope equipped with a 5Mp AmScpoe MD500 USB camera.

For liquid crystal MBBA, the condition $\varepsilon_{\parallel} < \varepsilon_{\perp}$ is fulfilled. In addition, the electrical conductivity in the direction parallel to the director ($\sigma_{\parallel}$) is larger than the conductivity in the direction perpendicular to the director ($\sigma_{\perp}$): $\sigma_{\parallel} > \sigma_{\perp}$. When these conditions are met and just above a certain critical voltage U_{th}, EHDI in the form of Williams domains are observed (Fig. 5) [16]. Williams domains are observed only at low frequencies and the threshold voltage of occurrence of these domains grows strongly with increasing frequency (Fig.6). Starting from a certain frequency (cutoff frequency) the observation of Williams domains becomes impossible.
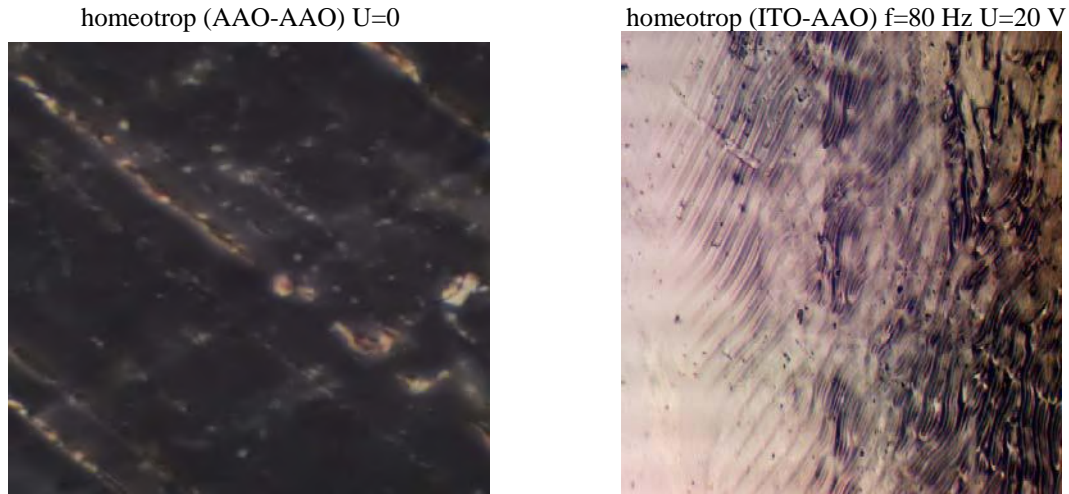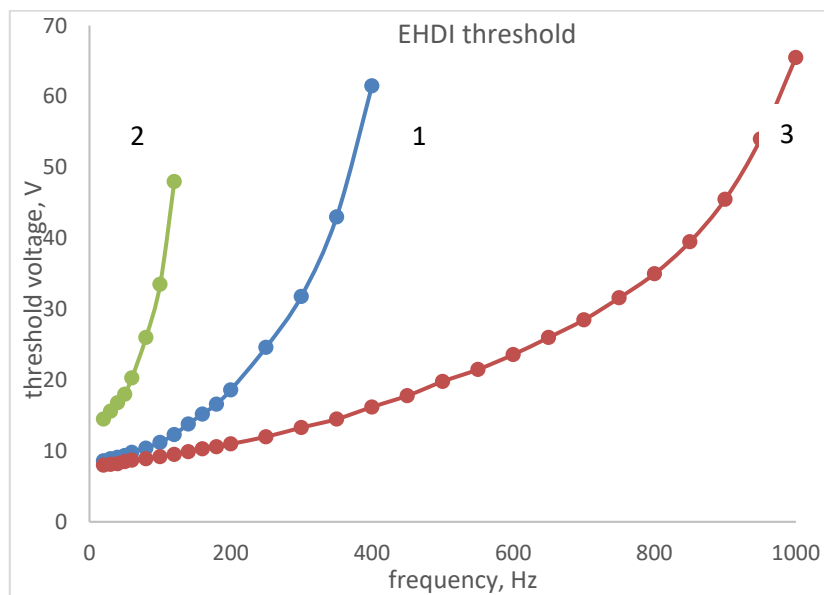
H37 (ITO-ITO) U=0 V

H37 (ITO-ITO) f=100 Hz U=20 V

hybrid (ITO-AAO) U=0

hybrid (ITO-AAO) f=150 Hz U=30 V

homeotrop (AAO-AAO) U=0

homeotrop (ITO-AAO) f=80 Hz U=20 V

Fig. 5

Fig. 6. 1 – ITO/ITO, 2 – ITO/AAO, 2 – AAO/AAO

RESULTS AND DISCUSSIONS

The results of measurements, i.e. frequency dependences of the threshold voltage of Williams domains occurrence for each cell of planar (ITO/ITO), hybrid (ITO/AAO) and homeotropic cell (AAO/AAO) are shown in Figure 6.

From the plots obtained, the following conclusions can be drawn:

1) compared to the planar cell (both ITO surfaces are untreated), in the hybrid cell (one surface is untreated and the other surface is coated with AAO) domains occur at low voltages and the cutoff frequency of the domains is noticeably higher;

2) in a homeotropically oriented cell (both surfaces are coated with AAO) Williams domains occur at high voltages, and the cutoff frequency is strongly reduced;

3) in a homeotropically oriented and hybrid cell, Williams domains have a complex structure, while the periodicity is observed.

To discuss the results, we briefly discuss the phenomenon of EHDI in liquid crystals and the theory of this phenomenon. This instability is observed at the case of alternating current with frequency not exceeding the inverse dielectric relaxation time $\omega = \dfrac{\sigma}{\varepsilon_0 \varepsilon}$, where ε and σ - dielectric permittivity and electrical conductivity of liquid crystal, respectively, and $\varepsilon_0 = 8,85\ pF\,/\,m$ is the electrical constant. If a low-frequency sinusoidal voltage is applied to a cell with a sufficiently conducting liquid crystal and negative dielectric anisotropy, then a regular pattern of vortex motion of the liquid in the form of long cylindrical rolls [14] perpendicular to the director appears. The instability occurs in cells of thickness $d = 10^{-5} - 10^{-4}\ m$ with a weakly thickness-independent threshold voltage. Such periodically arranged rolls are called Williams domains. In the polarization microscope Williams domains appear as well-defined parallel strips if the planar texture is sufficiently homogeneous. When the polarizer axis is

parallel to the director, the pattern is sharpest and forms a diffraction pattern with a period of the order of the cell thickness.

According to the Carr-Helfrich model [14], the cause of Williams domains is the destabilizing moment of viscous flow, which is associated with the anisotropy of electrical conductivity. The threshold voltage of the appearance of Williams domains is found from the balance of viscous, elastic and dielectric moments and is determined by the expression [16]

$$U_{th}^{EHDI} = \frac{\pi^2 K_{33}}{\Delta\varepsilon\varepsilon_0 \frac{\sigma_\perp}{\sigma_{//}} - \frac{\varepsilon_0\varepsilon_{//}\gamma}{\eta}\left(\frac{\varepsilon_\perp}{\varepsilon_{//}} - \frac{\sigma_\perp}{\sigma_{//}}\right)}$$

K_{33} is the elastic constant of bend deformation, η and γ are Leslie coefficients (simplified names translational and rotational viscosities, respectively). For LC with a small value of dielectric anisotropy ($\Delta\varepsilon << \varepsilon_{av}$) the formula takes a simplified form

$$U_{th}^{EHDI} = \sqrt{\frac{\pi^2 K_{33}\sigma_{//}\eta}{\alpha_2\varepsilon_0\varepsilon_{av}\Delta\sigma}}$$

As noted, when the LC is bordered by AAO on both sides, a homeotropic alignment with high anchoring energy is obtained. In this case, the EHDI is preceded by a transition from the homeotropic to the planar state in the form of an B-effect with a threshold voltage of 3.5 V [30]. Immediately above the threshold, only molecules in the middle of the sample rotate. As the voltage increases, the thickness of the planar layer increases. And EHDI is possible only if the thickness of this planar layer exceeds some critical value comparable to the thickness of the cell itself (LC layer), which requires sufficiently high voltages. Therefore, the EHDI threshold voltage for a cell where the LC is bounded on both sides by AAO (curve 2) is significantly higher than for a cell where the LC is bounded by ITO (curve 1).

The strong lowering of the threshold in the case of the hybrid cell is, in our opinion, related to the flexoelectric polarization [14], which plays a destabilizing role in this phenomenon.

Careful consideration of the micrographs (Figure 5) taken in the polarization microscope shows that in the homeotropically oriented and hybrid cells the Williams domains have a complex structure, but the periodicity is observed. This suggests a different dynamical distribution of the director due to the rigid normal anchoring of LC molecules to AAO.

CONCLUSION

Thus, if an anodized aluminum oxide is created on the electrodes in an electro-optic cell, then the threshold voltage of current effects (in this case, electro-hydrodynamic instabilitiy) in liquid crystal with negative dielectric anisotropy is drastically increased. This result has important implications for display applications similar liquid crystals.

_____

[1] *G.P. Crawford, S. Žumer*. Liquid crystals in complex geometry: Formed by polymer and porous networks, Taylor & Francis, 1996, 524 p.

[2] *M. Kleman, O.D. Lavrentovich*. Introduction to Soft Matter Physics: An Introduction, Springer-Verlag, 2003, 664 p.

[3] *R. Stannarius, F. Kremer*. Liquid Crystals in Confining Geometries, Lecture Notes in Physics, 2004, v.634, pp.301-336.

[4] *Y. Fomin*. Liquid. Crystal Defects in Confined Geometries, Supervisor Report, 2019, 43p.

[5] *J. Hardouin*. Active Liquid Crystals in Confinement, PhD Thesis, 2019, 227p.

[6] *Y. Gao*. Liquid Crystal Confined in Silica Nanoporous, Ph. D Thesis, The University of Tennessee, 2005

[7] *Z. Sumera, F. A. Fernandez, A. Striolo*. Liquid crystal droplets under extreme confinement probed by a multiscale simulation approach, Liquid Crystals, 2021, v. 48, No. 13, 1827–1839

[8] *Y. Li, JJ-Y Suen, E. Prince, et al.* Colloidal cholesteric liquid crystal in spherical confinement. Nat Commun. 2016; 7(1):1–11.

[9] *M. Kuzma, M.M. Labes*. Liquid Crystals in Cylindrical Pores: Effects on Transition Temperatures and SinguIarities, *Mol. Cvsr. Liq. Cryst.*, 1983, v. 100, 103-110.

[10] *E. Prince, Y. Wang, I. Smalyukh, E. Kumacheva*. Cylindrical Confinement of Nanocolloidal Cholesteric Liquid Crystal, J. Phys. Chem. B, 2021, 125, 8243-8250.

[11] *F.M. Aliev, G.P. Sinha*. Heterogenius mirocomposite materials based on porous matrices and liquid crystals - Materials Research Society Symposium Proceedings. Vol. 431, pp. 505-510.

[12] *F.M. Aliev, Z. Nazario, G.P. Sinha*. Broadband dielectric spectroscopy of confined liquid crystals, Journal of Non-Crystalline Solids 305 (2002) 218–225.

[13] *K. Sentker, A. Yildirim, M. Lippmann, A.W. Zantop, F. Bertram, T. Hofmann, O.H. Seeck, A.V. Kityk, M.G. Mazza, A. Schönhals, P. Huber*. Self-assembly of liquid crystals in nanoporous solids for adaptive photonic metamaterials, Nanoscale, 2019, 11, 23304-23317.

[14] *De Gennes P. G and J. Prost.* The Physics of Liquid Crystals, Oxford University Press, New York 1993.

[15] *L. Blinov.* Structure and Propertis of liquid Crystals, Springer, Heidelberg, London, New York, -2011. p.458.

[16] *L.M. Blinov, V.G. Chigrinov.* Electrooptic Effects in Liquid Crystal Materials Springer, Science & Business Media, New York, -1996. p.464.

[17] *D. Coates.* Polymer-dispersed Liquid Crystals, J. MATER. CHEM., 1995, 5(12), 2063-2072 2063

[18] *P.S. Drzaic*, Electro-Optics of Polymer-Dispersed Liquid Crystal Materials, Materials Research Society Symp. Proc. Vol. 425 01996, 259-268.

[19] *A. K. Jain, R.R. Deshmukh*. An Overview of Polymer-Dispersed Liquid Crystal Composite Films and Their Applications, DOI: http://dx.doi.org/10.5772/intechopen.91889

[20] *X.H. Wang, T. Akahane, H. Orikasa and T. Kyotani,* Brilliant and tunable color of carbon-coated thin anodic aluminum oxide films. Appl. Phys. Lett. 200791 011908

[21] *A.A. Lutich, S.V. Gaponenko, N.V. Gaponenko, L.S. Molchan, V.A. Sokol and A.V. Parkhutik.* Anisotropic light scattering in nanoporous materials: a photon density of states effect Nano Lett V 2004. 4, 1755–1782.

[22] *Sh.O. Eminov, A.M. Hashimov, A.A. Rajabli, A.X. Karimova,* Integration of Electrical Energy Storage Devices with Photovoltaic Solar Cells in One Hybrid System. In: S. Krishnamoorthy, K. Iniewski, ((eds) Advances in Fabrication and Investigation of Nanomaterials for Industrial Applications. Springer, Cham. (2024). https://doi.org/10.1007/978-3-031-42700-8_18

[23] *U. Cigane, A. Palevicius, G. Janusas,* Vibration-Assisted Synthesis of Nanoporous Anodic Aluminum Oxide (AAO) Membranes, Micromachines (Basel), 2022, 13(12):2236. doi: 10.3390/mi13122236.

[24] *A. Ganapathi, P. Swaminathan and L. Neelakantan.* Anodic Aluminum Oxide Template Assisted Synthesis of Copper Nanowires using a Galvanic Displacement Process for Electrochemical Denitrification *ACS Appl. Nano Mater.* 2019, 2, 9, 5981–5988.

[25] *S. Liu J. Tian, W. Zhang.* Fabrication and application of nanoporous anodic aluminum oxide: A review, Nanotechnology, 2021,32(22), 1-18, DOI: 10.1088/1361-6528/abe25f

[26] *T. Maeda and K. Hiroshima.* Vertically aligned nematic liquid crystal on anodic porous alumina, Japan. J. Appl.Phys., 2005, 43, L1004–6.

[27] *T.T Tang, C.Y Kuo, R.P. Pan, J.M. Shieh and C.L. Pan.* 2009. Strong vertical alignment of liquid crystal on porous anodic aluminum oxide film J. Disp. Technol. 5 350–4.

[28] *Ch. Hong, T.T. Tang, C.Y. Hung, R.P. Pan and W. Fang.* Liquid crystal alignment in nanoporous anodic aluminum oxide layer for LCD panel applications, Nanotechnology, 21,2010, 285201-285210.

[29] *T.T. Tang, Ch.Y. Hung, R.P. Pan, Ch. Hong, W. Fang.* Vertical Alignment of Liquid Crystal on ITO Glass with Anodic Aluminum Oxide Thin Film, Mol. Cryst. Liq. Cryst., 2011, Vol. 543: pp. 926–934.

[30] *T.D. Ibragimov, A.R. Imamaliyev, G.M. Bayramov.* Influence of barium titanate particles on electro-optic characteristics of liquid crystalline mixture H-37,Optik, 2016, 1217-1220.